Journal of Marine Research, 42, 303–317, 1984

A continental shelf upwelling event off Vancouver Island as revealed by satellite infrared imagery

by M. Ikeda[1,2] and W. J. Emery[1]

ABSTRACT

A series of nine relatively cloud-free infrared satellite images, of the coastal ocean off Vancouver Island, reveals the evolution of sea-surface temperature patterns during a 16-day period of upwelling favorable winds in the summer of 1980. Early in the upwelling event, the cold water in the north was restricted to a narrow band, while in the south cold surface water extended out to the continental shelf break. This southern feature is believed to be an expression of a semipermanent, cold cyclonic eddy (Freeland and Denman, 1982). As upwelling continued, the cold water boundary propagated offshore at about 10 km/day eventually passing beyond the shelf break. Short-lived (2–3 days) meanders were observed in the northern front with length scales consistent with variations in local bottom topography and coastline irregularities. After wind reduction, the coldest band parted the coast and propagated offshore.

1. Introduction

A northwesterly wind blows along the coast of Vancouver Island in summer, promoting coastal upwelling over the continental shelf as reported by Freeland and Denman (1982). Their hydrographic and current meter observations revealed seasonal variations in the coastal upwelling. In the present paper sea-surface temperature patterns, as depicted by a series of infrared satellite images, demonstrate the short-period (2 weeks) evolution of this wind-driven coastal upwelling.

Coastal upwelling has been observed and studied more extensively off Oregon and northwest Africa (see Holladay and O'Brien, 1975; Huyer, 1976; and Barton *et al.*, 1977). An upwelling event, corresponding to variations in wind forcing with a time scale of a few weeks, starts with cold sea-surface temperature near the coast within a day after the initial wind increase. This cold region near the coast expands offshore at a speed of 5 ~ 10 km/day. In addition to this transient upwelling, a continuous rise of subsurface isotherm has been observed near the coast of Oregon during the season when upwelling favorable winds blow (Huyer *et al.*, 1974). This continuous upwelling has also been seen over the European continental shelf break (Dickson and Gurbutt, 1980).

These transient and continuous upwelling events were simulated by various theoreti-

1. Department of Oceanography, University of British Columbia, Vancouver, B.C., Canada, V6T 1W5.
2. Present affiliation: Bedford Institute of Oceanography, Dartmouth, N.S., Canada, B2Y 4A2.

cal studies (Hurlburt and Thompson, 1973; Janowitz and Pietrafesa, 1980; and Hamilton and Rattray, 1978). From theory, long-lived (>15 days), upward fluid motion continues near the coast (within ~10 km) and over the shelf break. The isopycnal surface rise propagates from the coast, but the upward motion ceases within 10 days of the wind onset. Hence, a continuous cold sea surface should be observed only near the coast and over the shelf break, while a low temperature region propagates offshore extending beyond the shelf over a period of several days.

In this paper, a wind-driven upwelling event is presented as observed in nine infrared satellite images extending over 16 days. The satellite images exhibit the offshore propagation of a cold sea surface and the probable surface expression of shelf break upwelling. The wind-driven upwelling event apparently added to the surface expression of a cold cyclonic eddy located over the southern section of the Vancouver Island continental shelf. This eddy was discussed in detail by Freeland and Denman (1982).

2. Satellite imagery and wind data

Polar orbiting U. S. weather satellites (TIROSN and NOAA6) provided sea-surface thermal radiation data from the west coast of Vancouver Island under cloud-free conditions. Geometric distortions due to earth curvature, rotation and satellite attitude were corrected, using selected ground control points, to within 2 km. The study region is shown in Figure 1 with the latitude, longitude grid used and the 200 m isobath. In addition are shown the positions of the current meter moorings, and the wind stations where data used in this study were collected. A baseline, which nearly corresponds to the shelf break (200 m depth), is also included in Figure 1 (dark solid line) and will be used to measure the seaward propagation of the cold upwelling region and to analyze alongshore variability. The baseline, with a 270 km length, is divided into nine cross-shelf sections labelled A through I.

An upwelling event was observed in nine satellite images taken between July 21 and August 5, 1980. Before looking at the images, it is instructive to examine the corresponding wind data (Fig. 2). Note that Bakun's upwelling index, taken from Freeland and Denman (1982), is based on the wind data measured at the southern station (125W, 48N), which is ~200 km southeast of the northern station where the wind vectors, at the top of Figure 2, were observed. Hence, we can interpret the upwelling event only in terms of the wind variations which are common between the northern and southern regions. As is typical for summer the wind was mostly from the northwest. Around July 20 the wind was weak strengthening on July 23 to produce a maximum in the upwelling index. Following this increase there is a 5-day period (July 26–30) of large wind magnitudes. After this period, the wind reduced leading to a smaller upwelling index on August 1. This northwesterly wind event should induce transient, coastal upwelling.

The various stages of an upwelling event can be seen in the infrared satellite images (Fig. 3). In these images lighter grey shades correspond to colder radiation tempera-

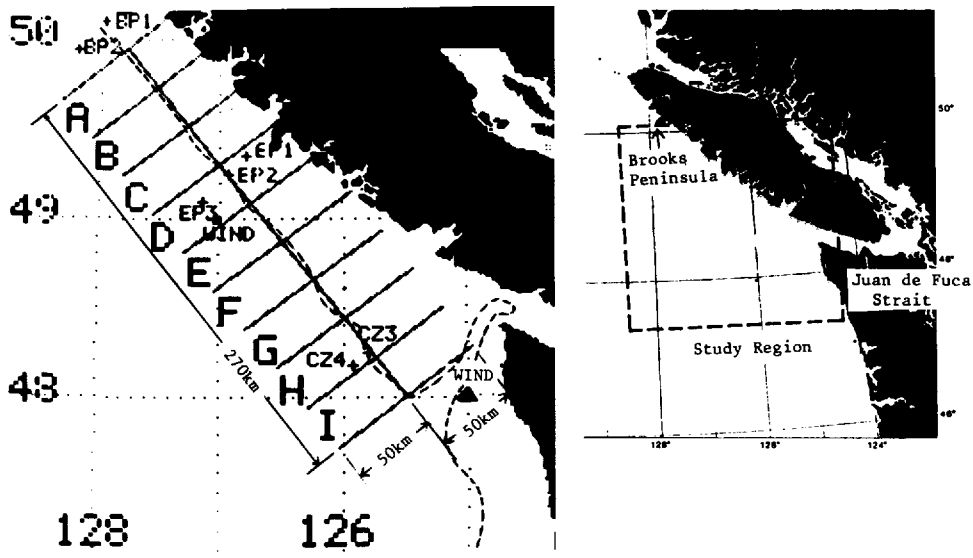

Figure 1. The area observed by satellite infrared images. Seven current meter mooring stations (BP1, BP2, EP1, EP2, EP3, CZ3, CZ4) are indicated by +, and the northern and southern wind stations by ■ and ▲, respectively. The baseline is indicated by a solid line, with lines perpendicular to the baseline. The 200 m isobath is shown by a broken line.

tures. The enhancement for all images was designed to set the lower left sea surface (cloud-free) as a reference level for the same linear grey shade transformation. Thus assuming that the study region was not subject to intense local heating and cooling events over the short time scale of study, it is reasonable to expect that light grey shades, over the shelf region, correspond to decreases in sea-surface temperature.

3. The upwelling event

a. Early stages of the upwelling event (July 21–26). On July 21, before the upwelling event, the coastal waters off Vancouver Island were generally warm (Fig. 3a). During this time the wind was weak and variable in direction (Fig. 2). In the southern coastal ocean off the mouth of Juan de Fuca Strait there is a patch of cold water at Sections H and I, (125–126W, 48–48.5N). The spiral shape of cold water, which may be thought of as a tracer, indicates cyclonic rotation associated with an eddy. As discussed by Freeland and Denman (1982), this eddy was generated by the combination of local topography and alongshore flow.

From July 21 to 23, the northwesterly wind strengthened to double the Bakun upwelling index (Fig. 2). In response to this upwelling favorable wind, the near-shore coastal temperatures appear colder on July 23 (Fig. 3b). This narrow band widened on July 24 and 26 (Figs. 3c, 3d) in the northern half (Sections C–F), while farther south (Sections G–I) the cold water boundary extended seaward out to the shelf break. This

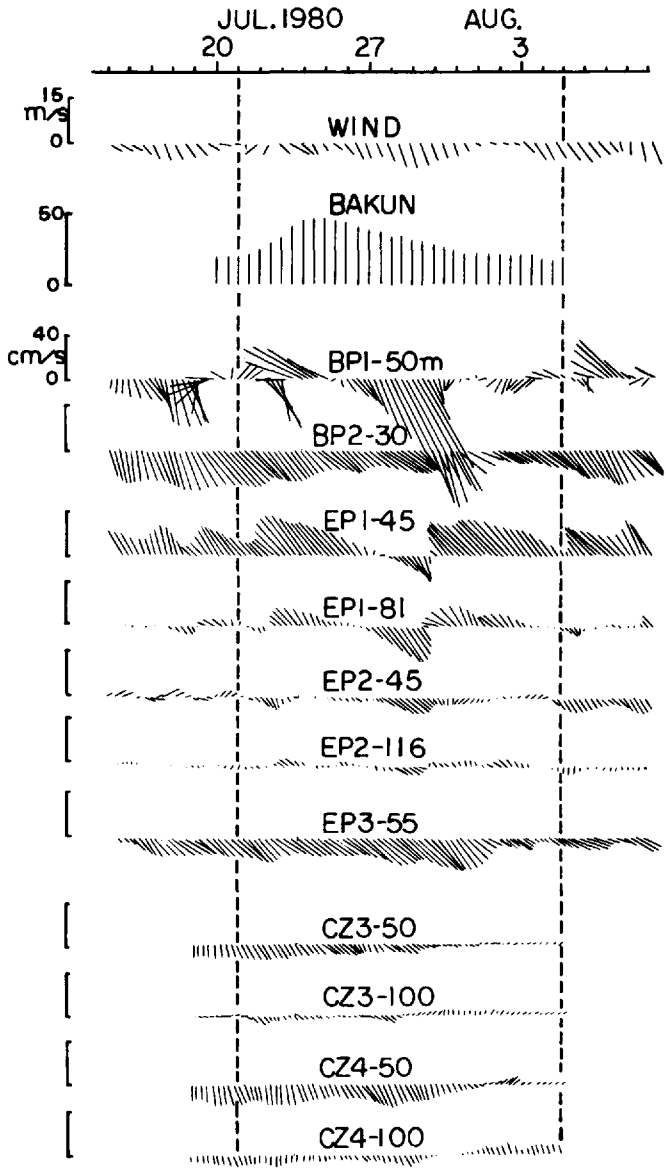

Figure 2. Wind data and current meter data collected at the seven mooring stations. All positions are indicated in Figure 1. The northern wind data (vectors) and current meter data at BP1–EP3 are courtesy of Drs. R. Thomson, S. Huggett and W. Crawford, and the other by Dr. H. Freeland at the Institute of Ocean Sciences, Sidney, B.C. Also, Bakun's upwelling index at the southern station was taken from Freeland and Denman (1982).

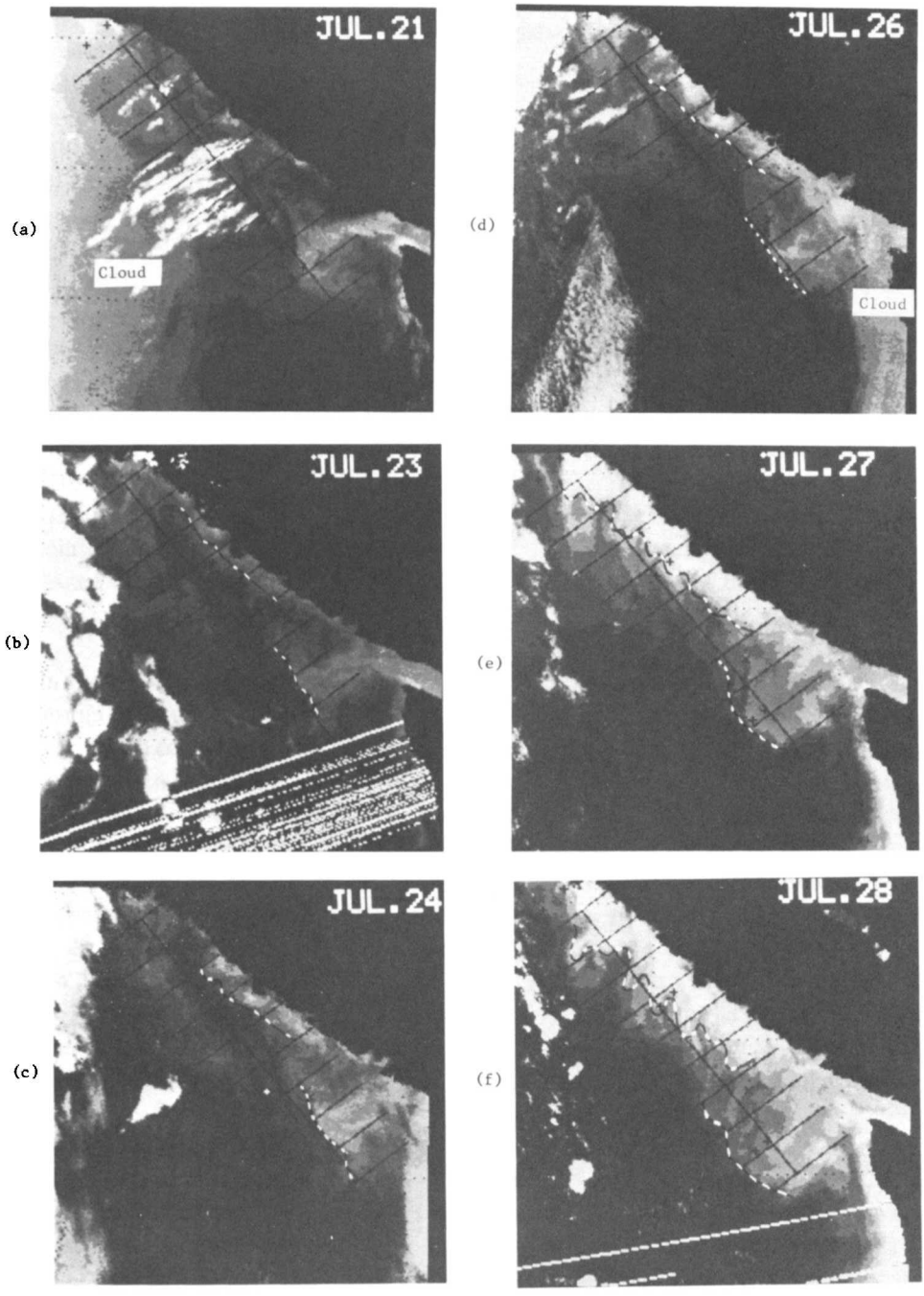

Figure 3. Satellite infrared images taken on (a) July 21, (b) 23, (c) 24, (d) 26, (e) 27, (f) 28, (g) 30 and (h) August 3, (i) 5 of 1980. The offshore boundaries of the upwelling region are indicated for the southern sections (-----) and the northern sections (———).

(g)

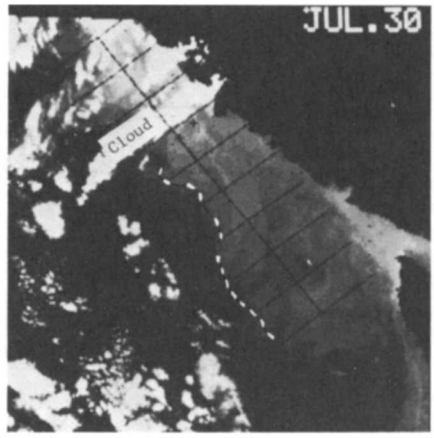

(h)

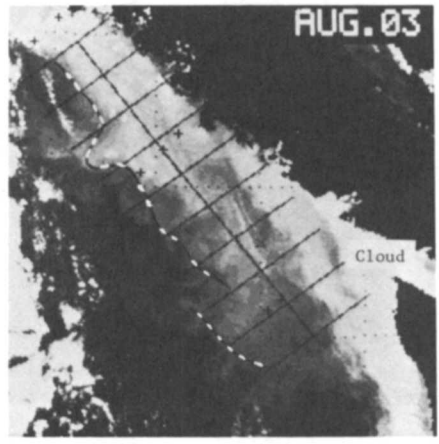

(i)

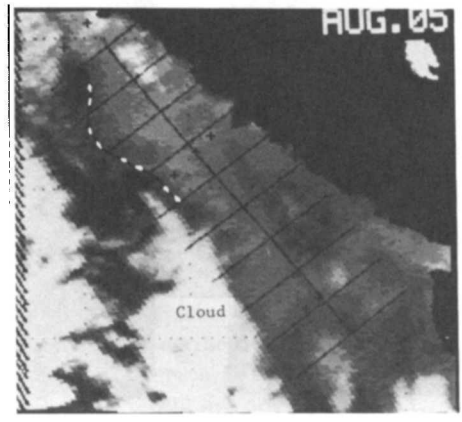

Figure 3. Continued.

southern cold pool is due at least in part to the cyclonic eddy discussed above. The influence of the wind-driven "upwelling" on the surface expression of this eddy can be seen throughout the sequence of satellite images.

In addition to the near coast, cold region, a separate cold band is observed offshore of the shelf break, extending from the north to Section E on July 23–26 (Figs. 3b–d). This band appears to be advected by the southward flow from the colder northern district, but could also be the expression of upwelling at the shelf break. It is unknown how much upwelled water contributed to this colder surface band.

The offshore boundaries of both the northern, near coast upwelling and the southern eddy/upwelling are plotted on the images in Figure 3. Here the boundaries are defined as the offshore edges of the frontal zones in which the horizontal temperature gradient is larger than 1.2°C/10 km (a three-increment difference in 8-bit radiation data).

In order to examine the character of the upwelling event more objectively, we have computed sea-surface temperature structures along the nine sections labelled A–I in Figure 1. Averaging the satellite infrared radiance data around each section parallel to the shelf, we obtain the structures shown in Figure 4a–e for July 24–August 3. Since no absolute temperature calibration was done, each curve is referenced to the same mean radiance using the warm, cloud-free region in the lower left of each image as the reference value. For comparison an equivalent temperature interval is shown in Figure 4a.

In the sea-surface temperature structures (Fig. 4) fronts, indicated by arrows, are determined as the positions of the steepest slopes. Only for very large temperature defects (deep concaves in the structure curves) at C ~ F of July 27 (Fig. 4c), A of July 28 (Fig. 4d) and A of August 3 (Fig. 4f), are the fronts taken to be the offshore edges of the steep (1°C/10 km) slopes. Since the structure is a 30 km average, the slopes are gentler than the local temperature gradients in the satellite images. The fronts determined from the structure curves are almost identical to the offshore boundaries of cold water plotted on the satellite images (Fig. 3), but, in some cases, are located 10 ~ 20 km closer-to-shore.

On July 24 and 26 (Fig. 4a, b), the fronts of the northern upwelling are located 10 ~ 30 km onshore of the shelf break or ~20 km seaward from the coast. The fronts associated with the southern cold region are seen around the shelf break. The offshore cold band (shelf break upwelling) is also clearly indicated by the small values at Sections A ~ E, 35–10 km offshore of the shelf break.

Let us look at the current meter data in Figure 2. Although the sea-surface temperature, as seen in the satellite images, indicates the start of upwelling on July 23, the current velocity shows no significant change until July 25. The southeastward vectors at moorings BP2 and EP3 indicate that the offshore cold band corresponds to the southeastward, near-surface current. The northwestward flow at EP1 implies the outflow of fresh water discharged from Juan de Fuca Strait and Vancouver Island, as Thomson *et al.* (1982) suggested.

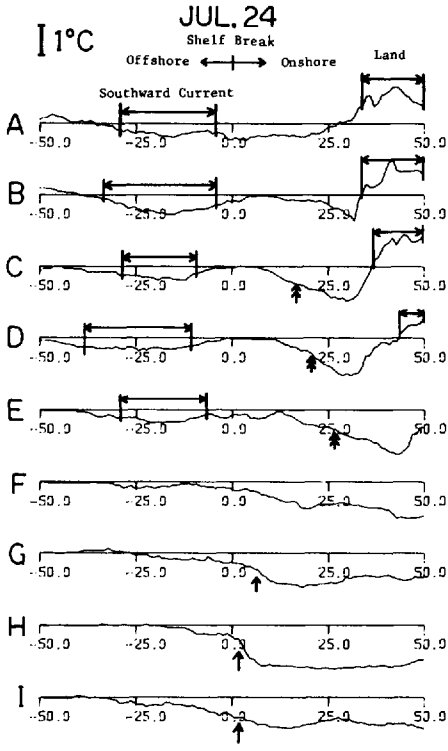
JUL. 24
1°C
Shelf Break
Offshore
Onshore
Land
Southward Current
A
B
C
D
E
F
G
H
I
-50.0
-25.0
0.0
25.0
50.0

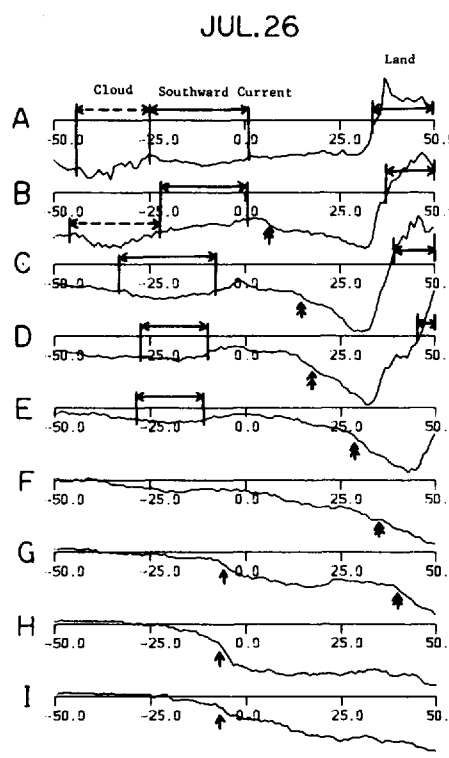
JUL. 26
Land
Cloud
Southward Current
A
B
C
D
E
F
G
H
I
-50.0
-25.0
0.0
25.0
50.0

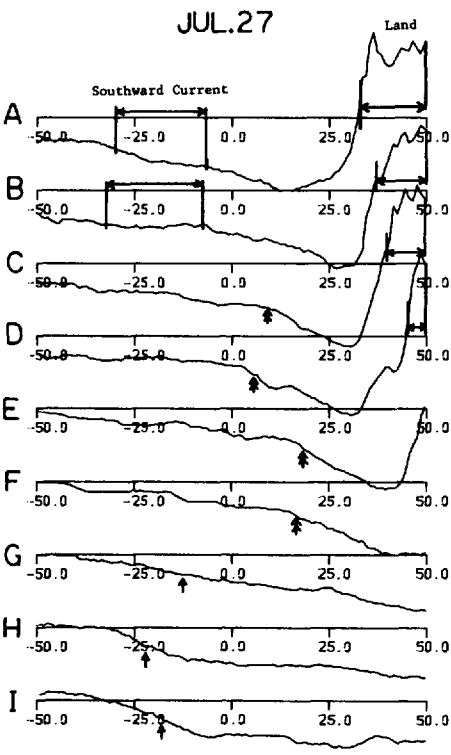
JUL. 27
Land
Southward Current
A
B
C
D
E
F
G
H
I
-50.0
-25.0
0.0
25.0
50.0

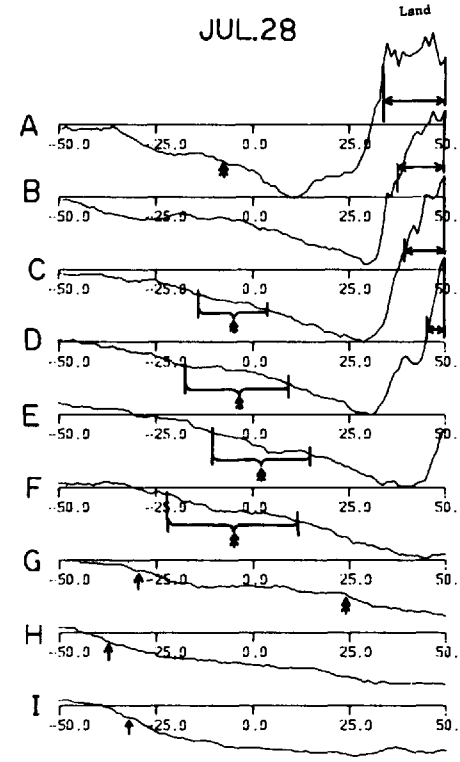
JUL. 28
Land
A
B
C
D
E
F
G
H
I
-50.0
-25.0
0.0
25.0
50.0

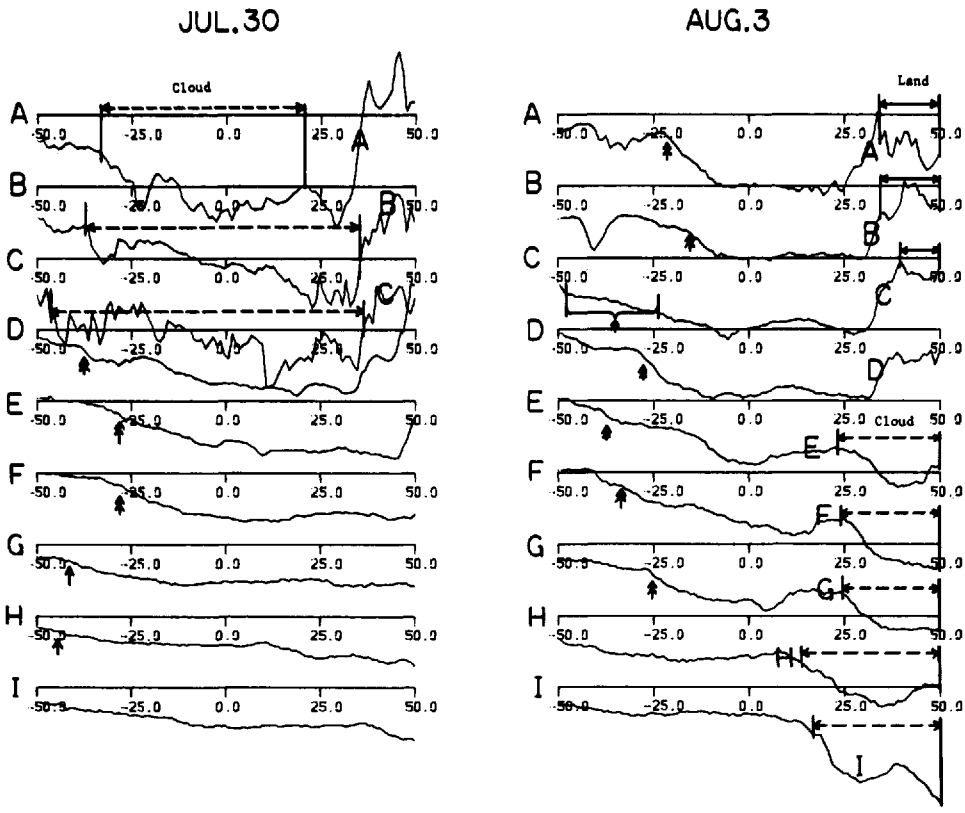

Figure 4. The onshore-offshore temperature distribution in each section for (a) July 24, (b) 26, (c) 27, (d) 28, (e) 30 and (f) August 3. Here the temperature indicates the deviation from the reference level far offshore from the shelf region. The origins of the horizontal axes correspond to the baseline shown in Figure 1, and the distance is measured by kilometers. The arrows and double arrows designate the fronts associated with the southern and northern upwelling regions, respectively.

b. Middle of the event (July 27–30). From the common features between the wind vectors and Bakun index in Figure 2 the northwesterly wind was the most intense between July 23 and 30 (Fig. 2). Up to the end of July the cold sea surface was expanding offshore (Fig. 3e–g). The northern, near coast upwelling region spread out over the entire shelf and connected with the offshore cold band by July 27. Of particular interest is the sharply meandered form of this boundary on July 27 and 28 as compared with the previous day (Fig. 3d). The meander amplitude grew between July 26 and 28, and these meanders broke down to allow horizontal mixing of the cold coastal waters, evidenced by a smoother front on July 30 (Fig. 3g).

The meandering pattern of the front at Sections C–F on July 28 (Fig. 3f) is compared with the alongshore variations of bottom topography and coastline irregular-

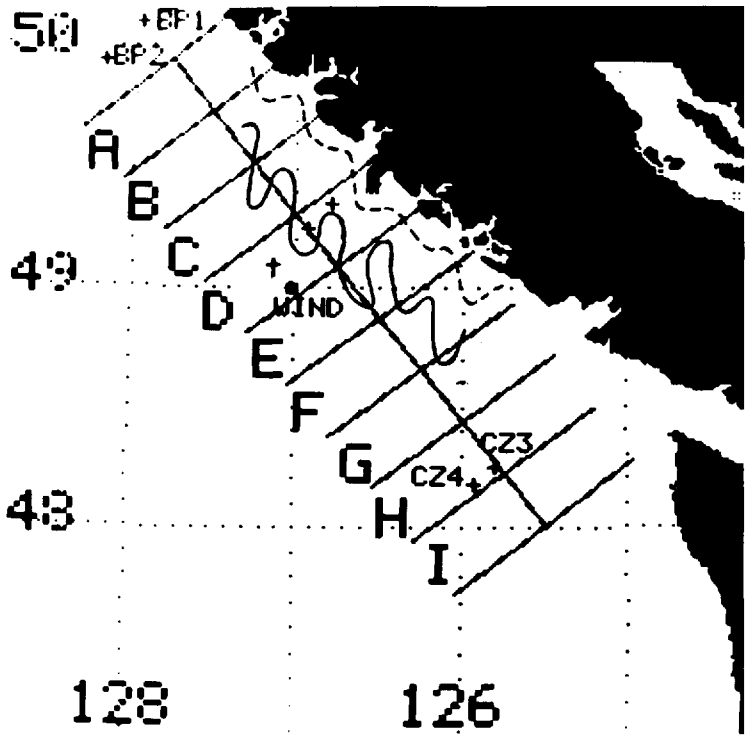

Figure 5. The boundary of colder sea surface on July 28. The 50 m isobath is shown by a broken line.

ity in Figure 5. The offshore extending bumps of the front seem to stretch from the submarine ridges (and the capes), and to be advected southward by the mean current.

Fourier components of the sea surface thermal data are computed along the 270 km base line and presented in Figure 6. In addition to larger scale variations with wavelengths of >60 km, a separate peak, indicated by arrows, appears at a 30 km wavelength only on July 28. This scale change supports the meander growth evidenced along the shelf-break on July 28. Since meanders are restricted to the shelf region on July 27, the 30 km peak is not seen in the Fourier components computed along the base line. Unfortunately, since cloud covered more than half of the region exhibiting the meandering front on July 30, Fourier analysis was not performed. However, the meanders obviously broke down after July 30.

Evidence of the frontal meandering is shown as the hatched area in the time versus cross-shelf distance diagram of Figure 7. In this plot the frontal positions revealed by the temperature structures in Figure 4 have been averaged for Sections C–E and G–I and plotted as a function of time. The dashed line indicates an offshore propagation speed of 10 km/day and parallels the average position lines up to July 30 during the time of upwelling favorable winds. After this time the wind weakened and the

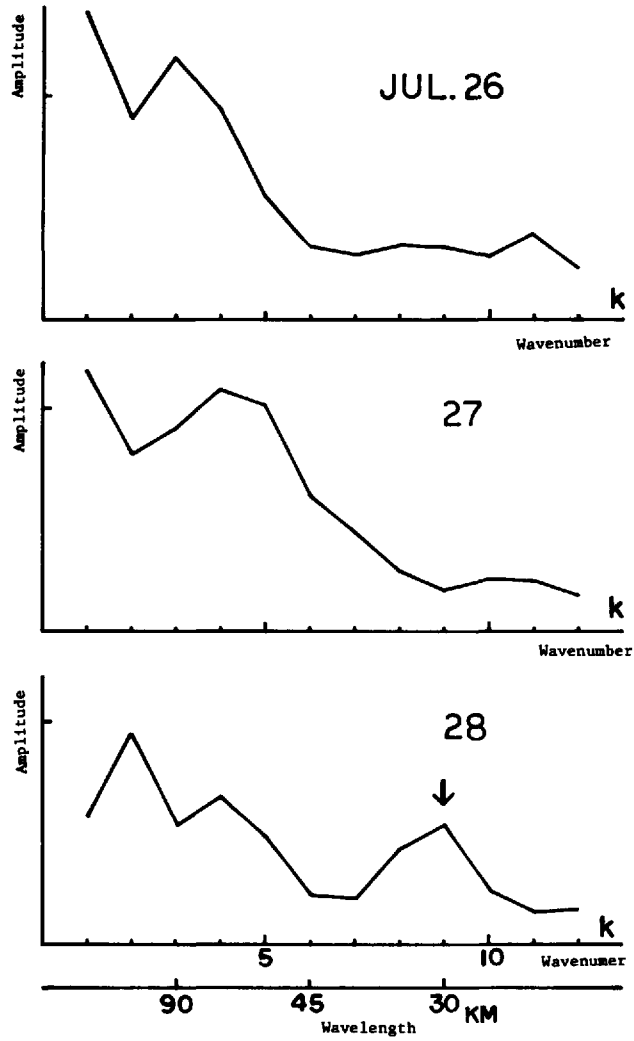

Figure 6. Fourier components of sea-surface thermal data along the baseline (Fig. 1) for (a) July 26, (b) 27 and (c) 28. k is a wavenumber in a 270 km-length of the baseline. Wavelengths are indicated below k.

propagation speed sharply reduced (change in slope) between July 30 and August 3, as discussed in Section 3c. The temperature decrease due to the upwelling event was ~2.5°C at a maximum on July 27 and 28 (Fig. 4c, d).

In addition to the northern upwelling region mentioned above, the cold surface water was spreading seaward in the southern sections G–I. The front reached out to 50 km offshore of the shelf break on July 30. The propagation speed was also ~10 km/day in this case (Fig. 7). Although the cyclonic eddy alone maintained a cold water pool at the

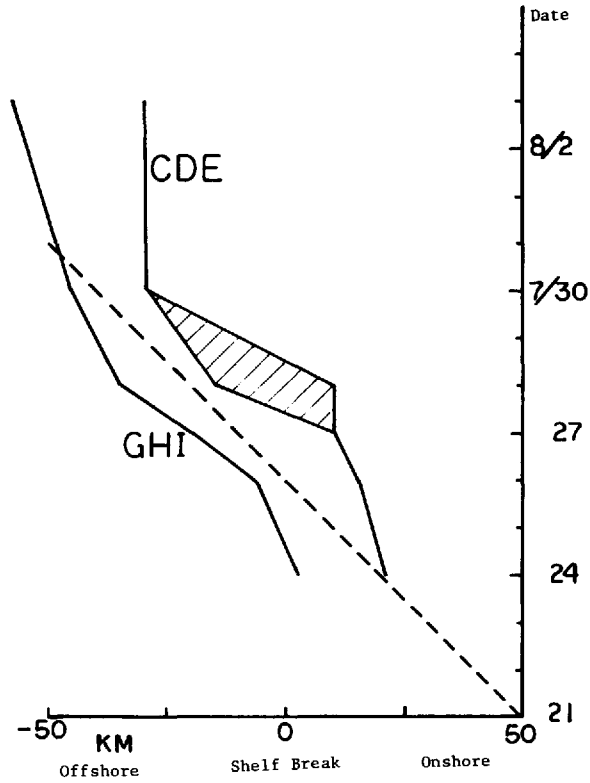

Figure 7. The front locations in a time-cross shelf distance diagram. The locations for the northern and southern upwelling regions are represented by the averages in Sections C ~ E and G ~ I, respectively, taken from Figure 4. The broken line indicates an offshore velocity of 10 km/day.

beginning, wind-induced upwelling obviously caused the cold region to expand and spread offshore in the middle of the wind event.

Corresponding to the strongest northwesterly wind, the current system (Fig. 2) intensified its southeastward velocity (BP2-30, EP2-45), had a pulse-like southeastward component (BP1-50), or changed the direction from northwest to southeast (EP1). The southern data (CZ3, CZ4) show much weaker effects. The striking large current amplitude ~100 cm s^{-1} at BP1 may be influenced by the cape called Brooks Peninsula.

c. Final stage of the event (August 3–5). The wind reduced to near zero between July 30 and August 3 (Fig. 2). The Bakun upwelling index dropped to approximately half that at its maximum on July 24. During this time the fronts associated with both the northern and southern cold regions propagated seaward much slower than was observed in the middle of the event (July 27–30). In addition, a major difference in the

thermal pattern over the shelf is seen in the last two satellite images (Fig. 3h, 3i). The coldest band that was attached to the coast until July 28 separated from the coast and shifted to the shelf break on August 3. On August 5 warm sea-surface water appeared over the entire shelf, with a cold band only over the shelf break. The separation of the coldest band is indicated also by the minimum values in the temperature structures (Fig. 4f) around the shelf break, Sections E–G.

It is of interest that the cyclonic eddy is still observed at the same position (Sections H and I) on August 5 as on July 21 (Fig. 3a). This suggests that the eddy existed semipermanently even during the upwelling event.

On July 31, the current system returned to the previous conditions after a ~7 day period of intense southeastward flow. Only EP3 shows a peak on July 31, which corresponds nicely to the location of the front on July 30 (Fig. 3g). This correspondence suggests that the fastest alongshore current shifted together with the fronts.

4. Discussion

The upwelling event demonstrated in this paper underwent the following evolution: before a northwesterly wind increased its intensity, a cold band was observed over the continental shelf break only. Nearly simultaneous with the wind intensification, colder sea-surface temperatures began to appear near the coast. This cold band broadened, and the offshore boundary propagated seaward out to the shelf break at a speed of ~10 km/day. Over the southern portion of the shelf, the boundary of the cold region started to propagate offshore from the seaward edge of a semipermanent, cyclonic eddy. During the 7-day period of the most intense wind, the southeastward current displayed its maximum magnitudes. The surface temperature front often exhibited meanders with an alongshore scale similar to variations in bottom topography and coastline irregularity. These meanders existed only for 2–3 days, and then broke up, allowing mixing of the colder coastal water. After the reduction of the wind, the coldest band parted the coast and propagated offshore. A warm region appeared over the shelf region again. The temperature deficit at the surface in the upwelling region was ~2.5°C at its maximum.

This transient upwelling over the continental shelf has also been observed off Oregon and northwest Africa. Off Oregon, the front, determined from the steepest seaward temperature gradient, propagated at a speed of ~10 km/day (Holladay and O'Brien, 1975). Off northeast Africa, the speed was ~5 km/day (Barton *et al.*, 1977). In these two areas, the wind intensities were nearly the same in magnitude (10–15 ms^{-1}) during the events.

This difference in offshore propagation speeds between the two regions is qualitatively consistent with a seaward flow difference near sea surface; i.e., a 25 cm s^{-1} maximum off Oregon and a 15 cm s^{-1} maximum off northwest Africa (Huyer, 1976). This velocity difference was attributed to the difference in the surface layer thicknesses, which depended on stratification; i.e., the stronger stratification off

Oregon leads to a thinner surface layer, resulting in a larger offshore flow (Huyer, 1976). Since the stratification off Vancouver Island is similar to that off Oregon, and the wind was weaker off Vancouver Island (7–10 ms^{-1}), the observed offshore propagation speed of the upwelling region, 10 km/day, is surprisingly large.

The cold band observed offshore before and at the early stages of the upwelling event (July 21–26) might represent shelf break upwelling. Another interpretation could be the southeastward advection of colder water from the north. Thus, it is unknown how much the upwelled water contributed to this colder surface feature. The continuous upwelling near the coast, observed off Oregon, may not be always represented by a corresponding decrease in sea-surface temperature. Hence, infrared satellite imagery is not capable of resolving this continuous upwelling.

It was observed herein that the upwelling front displayed transient meanders, the alongshore scale of which was similar to that of bottom variability and coastline irregularity. The effects of this topography on upwelling have been studied in various theoretical papers (Peffley and O'Brien, 1976; Killworth, 1978; Preller and O'Brien, 1980). The meanders observed in the present event, with a life time of 2–3 days, cannot be explained by these theories for a quasi-steady state. Hence, although the meanders were apparently generated by the topography, further theoretical work is needed to explain this generation mechanism.

Acknowledgments. The authors wish to thank H. Freeland, R. Thomson, S. Huggett and W. Crawford of the Institute of Ocean Sciences (IOS), Sidney, B.C. for the unpublished current meter data. They would also like to thank the image processing group at the University of British Columbia for a convenient use of the facility and P. Lust and K. Barber for typing the manuscript. The digital images were supplied by the Edmonton Weather Centre of the Atmospheric Environment Service. The assistance of G. Schramm, B. Bowkett, B. Hume and J. Bullis, along with all those who helped supply these tapes is gratefully acknowledged. The work reported here was supported by two Strategic Grants to L. A. Mysak and W. J. Emery from Canadian Natural Sciences and Engineering Research Council. One of the authors (M. I.) worked as a Research Associate of the University of British Columbia while this investigation was carried out.

REFERENCES

Barton, E. D., A. Huyer and R. L. Smith. 1977. Temporal variation observed in the hydrographic regime near Cabo Corveiro in the northwest African upwelling region, February to April 1974. Deep-Sea Res., *24,* 7–23.

Dickson, R. R. and P. A. Gurbutt. 1980. Satellite evidence of enhanced upwelling along the European continental slope. J. Phys. Oceanogr., *10,* 813–819.

Freeland, H. J. and K. L. Denman. 1982. A topographically controlled upwelling center off southern Vancouver Island. J. Mar. Res., *40,* 1069–1093.

Hamilton, P. and M. Rattray, Jr. 1978. A numerical model of the depth-dependent, wind-driven upwelling circulation on a continental shelf. J. Phys. Oceanogr., *8,* 437–457.

Holladay, C. G. and J. J. O'Brien. 1975. Mesoscale variability of sea surface temperatures. J. Phys. Oceanogr., *5,* 761–772.

Hurlburt, H. E. and J. D. Thompson. 1973. Coastal upwelling on a β-plane. J. Phys. Oceanogr., *3,* 16–32.

Huyer, A. 1976. A comparison of upwelling events in two locations: Oregon and Northwest Africa. J. Mar. Res., *34,* 531–546.

Huyer, A., R. L. Smith and R. D. Pillsbury. 1974. Observations in a coastal upwelling region during a period of variable winds. (Oregon coast, July 1972). Téthys, *6,* 1–2.

Janowitz, G. S. and L. J. Pietrafesa. 1980. A model and observations of time-dependent upwelling over the mid-shelf and slope. J. Phys. Oceanogr., *10,* 1574–1583.

Killworth, P. D. 1978. Coastal upwelling and Kelvin waves with small longshore topography. J. Phys. Oceanogr., *8,* 188–205.

Peffley, M. B. and J. J. O'Brien. 1976. A three-dimensional simulation of coastal upwelling off Oregon. J. Phys. Oceanogr., *6,* 164–180.

Preller, R. and J. J. O'Brien. 1980. The influence of bottom topography on upwelling off Peru. J. Phys. Oceanogr., *10,* 1377–1398.

Thomson, R. E., H. J. Freeland and W. R. Crawford. 1982. Circulation of the British Columbia shelf region: some recent advances. (Abstract) EOS, *63,* 1007.

Received: *10 May, 1983;* revised: *17 November, 1983.*